

Synthesis and Properties of New Chromium(II) Organophosphonates

Carlo Bellitto* and Fulvio Federici

Istituto di Chimica dei Materiali del C.N.R., Area della Ricerca di Roma, C.P.10, Via Salaria Km.29.5, I-00016 Monterotondo Staz., Roma, Italy

Said A. Ibrahim

Department of Chemistry, Faculty of Science, Assiut University, Egypt

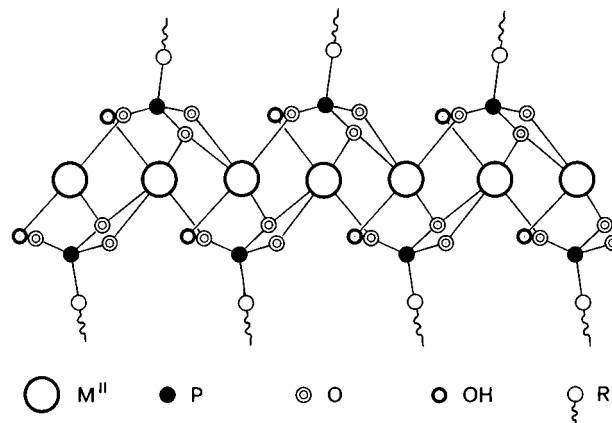
Received October 2, 1997. Revised Manuscript Received January 28, 1998

A new series of chromium(II)-alkylphosphonates, $\text{Cr}[\text{RPO}_3] \cdot \text{H}_2\text{O}$ ($\text{R} = \text{CH}_3, \text{C}_2\text{H}_5$), and chromium(II) ethylenebis(phosphonate), $\text{Cr}_2[\text{O}_3\text{P}-(\text{CH}_2)_2-\text{PO}_3] \cdot 3\text{H}_2\text{O}$, have been synthesized by reaction of CrCl_2 and the corresponding phosphonic acid in water in the presence of urea. The (2-aminoethyl)phosphonic acid reacts with CrCl_2 to give an unexpected compound of formula $\text{Cr}[\text{H}_3\text{N}-(\text{CH}_2)_2-\text{PO}_3(\text{Cl})]$. All the compounds are sensitive to the air, except for the latter one. They were characterized by X-ray powder diffraction, thermogravimetry, and UV-visible and infrared spectroscopy, and their magnetic properties were studied by a SQUID magnetometer. The metal ion is in the high-spin d^4 configuration, and it appears to have an octahedral coordination. $\text{Cr}[\text{CH}_3\text{PO}_3] \cdot \text{H}_2\text{O}$ behaves as a "weak" ferromagnet, with a Néel temperature of $T_N = 35$ K, and it represents an example of an unusual kind of molecular-based magnetic material, having a finite zero-field magnetization. The thermal variation of the magnetic susceptibility of $\text{Cr}_2[\text{O}_3\text{P}-(\text{CH}_2)_2-\text{PO}_3] \cdot 3\text{H}_2\text{O}$ follows the Curie-Weiss law, with a large negative Weiss constant of $\theta = -73$ K. Below 100 K, the susceptibility increases until a peak at $T_N = 15$ K is observed, and this is associated to the three-dimensional antiferromagnetic order. $\text{Cr}[\text{H}_3\text{N}-(\text{CH}_2)_2\text{PO}_3(\text{Cl})]$ is paramagnetic down to 5 K.

Introduction

Metal phosphonates, $\text{M}[\text{RPO}_3] \cdot \text{H}_2\text{O}$,^{1a} and bis(phosphonates), $\text{M}_2[\text{O}_3\text{P}-\text{R}-\text{PO}_3] \cdot n\text{H}_2\text{O}$ ^{1b} (M is a divalent metal ion and R is an alkyl or aryl group) are interesting materials because they can be used as ionic exchangers,² catalysts,³ and hosts in intercalation compounds.^{4,5} $\text{M}^{\text{II}}[\text{RPO}_3] \cdot \text{H}_2\text{O}$,^{4a} ($\text{M} = \text{Cd}, \text{Mn}, \text{Fe}, \text{Co}, \text{Ni}, \text{Zn}$) crystallizes mainly in a layered structure, composed of metal ions and the phosphonate oxygen atoms lying in puckered sheets. The pendent organic R groups lie in the interlamellar space, and two organic layers, having van der Waals contacts, are interspersed to the inorganic ones (see Scheme 1). The bonding requirements of the metal ion determine the atomic arrangement within these

Scheme 1



(1) (a) For a recent review, see for example: Alberti, G. In *Comprehensive Supramolecular Chemistry*; Atwood, J. L., Davies, J. E. D., Macnicol, D. D., Vogtle, F., Eds.; Pergamon Press: New York, 1996; Vol. 7, p 151 and references therein. (b) Poojary, D. M.; Zhang, B.; Bellinghausen, P.; Clearfield, A. *Inorg. Chem.* **1996**, *35*, 5254. (c) Bonavia, G.; Haushalter, R. C.; O'Connor, C. J.; Zubieta, J. *Inorg. Chem.* **1996**, *35*, 5603.

(2) Kullberg, L.; Clearfield, A. *Solvt. Extn. Ion Exch.* **1989**, *7*, 527. (3) Centi, G.; Trifirò, F.; Ebner, J. R.; Franchetti, V. M. *Chem. Rev.* **1988**, *88*, 125.

(4) (a) Cao, G.; Lee, H.; Lynch, V. M.; Mallouck, T. E. *Inorg. Chem.* **1988**, *27*, 2781. (b) Cao, G.; Mallouck, T. E. *Inorg. Chem.* **1991**, *30*, 1434. (c) Zhang, Y.; Scott, K. J.; Clearfield, A. *Chem. Mater.* **1993**, *5*, 495.

(5) (a) Johnson, J. W.; Jacobson, A. J.; Brody, J. F.; Lawandowsky, J. T. *Inorg. Chem.* **1984**, *23*, 3842. (b) Johnson, J. W.; Jacobson, A. J.; Butler, W. M.; Rosenthal, S. E.; Brody, J. F.; Lewandowsky, J. T. *J. Am. Chem. Soc.* **1989**, *111*, 381. (c) Huan, G. E.; Jacobson, A. J.; Johnson, J. W.; Corcoran, E. W. *Chem. Mater.* **1990**, *2*, 91. (d) Johnson, J. W.; Brody, J. F.; Jacobson, A. J.; Alexander, R. M.; Pilarski, B.; Katritzky, A. R. *Chem. Mater.* **1990**, *2*, 198.

inorganic layers. In copper phosphonates, $\text{Cu}[\text{RPO}_3] \cdot \text{H}_2\text{O}$ ($\text{R} = \text{CH}_3, \text{C}_2\text{H}_5, \text{C}_6\text{H}_5$), the metal ion is five-coordinated, in a distorted tetragonal pyramidal symmetry. The base of the pyramid consists of three phosphonate oxygens and a coordinated water molecule. The three oxygens of the phosphonate groups are all bonded to the Cu atoms with two of them bridging copper atoms.^{6,7} The organic groups are pointing toward the interlamellar space above the $[\text{CuO}_3\text{P}]$ inorganic layers, making

(6) Zhang, Y.; Clearfield, A. *Inorg. Chem.* **1992**, *31*, 2821.

(7) (a) Le Bideau, J.; Palvadeau, P.; Payen, C.; Bujoli, B. *Inorg. Chem.* **1994**, *33*, 4885. (b) Maeda, K.; Akimoto, J.; Kiyozumi, Y.; Mizukami, F. *Angew. Chem., Int. Ed. Engl.* **1995**, *34*, 1199. (c) Lohse, D. L.; Sevov, S. L. *Angew. Chem., Int. Ed. Engl.* **1997**, *36*, 1619.

van der Waals contacts between layers. Manganese(II), iron(II), cobalt(II), and zinc(II), on the other hand, are six-coordinated.^{8,9} The metal ion is again surrounded by a very low symmetry coordination of oxygens, five from the phosphonate groups and one from the water molecule. A lamellar structure has also been observed in many metal bis(phosphonates).¹ The inorganic layers, viewed end on, have a zigzag appearance, with the P atoms above and below the plane of the layer at the crests and the water molecules at the troughs. These layers are bridged by the organic groups of the ligands to give a 3D structure. Moreover, an interesting phase of the anhydrous copper methylphosphonate has also been isolated, i.e., the β -form. The copper ion is still in a distorted tetragonal pyramidal coordination, and the resulting 3D structure shows an interesting honeycomb network.^{7a} Similar microporous structures have been also recently observed in α -Al methylphosphonate^{7b} and in $\text{Co}_2[\text{O}_3\text{P}-\text{CH}_2-\text{PO}_3]\cdot\text{H}_2\text{O}$,^{7c} all characterized by having a channel-type arrangement. Finally, some metal phosphonates, containing open-shell metal ions, show cooperative magnetism at low temperatures. $\text{Cu}[\text{C}_n\text{H}_{2n+1}\text{PO}_3]$, $n = 1, 2, 3$, salts behave as 1D antiferromagnetic systems,^{6,7} while $\text{Mn}[\text{C}_n\text{H}_{2n+1}\text{PO}_3]\cdot\text{H}_2\text{O}$ ⁸ and $\text{Fe}[\text{C}_2\text{H}_5\text{PO}_3]\cdot\text{H}_2\text{O}$ ⁹ are weak ferromagnets. Cr(II) organophosphonates were not previously studied. Cr(II) ion (d^4 , $S = 2$) in an octahedral coordination is interesting from the magnetic point of view. It gives several examples of magnetic materials. As regards this, it is worth to mention ternary Cr(II) halides, $(\text{RNH}_3)_2\text{CrX}_4$, having a layered perovskite structure, were found to be ferromagnets with the critical temperature, T_c , around 50 K.¹⁰ With this in mind and with the aim of synthesizing new insulators, which might order ferromagnetically, we have prepared and characterized a new series of chromium(II) organophosphonates and studied their magnetic properties. Phosphonates having different organic and functionalized groups were selected for this purpose. This paper reports the first systematic study of chromium(II) organophosphonates, i.e., $\text{Cr}[\text{C}_n\text{H}_{2n+1}\text{PO}_3]\cdot\text{H}_2\text{O}$, ($n = 1, 2$), $\text{Cr}_2[\text{O}_3\text{P}-(\text{CH}_2)_2-\text{PO}_3]\cdot 3\text{H}_2\text{O}$, and $\text{Cr}[\text{H}_3\text{N}-(\text{CH}_2)_2-\text{PO}_3(\text{Cl})]$.

A brief communication of the synthesis and magnetic studies of the methylphosphonate salt has been presented earlier.¹¹

Experimental Section

Materials and Methods. Alkylphosphonic acids, triethylphosphite (moisture-sensitive), and 1,2-dibromoethane were used as obtained from Aldrich Chemical Co., without further purification. HPLC water was used as solvent. The ethylenebis(phosphonic acid), $\text{H}_2\text{O}_3\text{P}-(\text{CH}_2)_2-\text{PO}_3\text{H}_2$, was prepared by the Michaelis–Arbuzov reaction of 1,2-dibromoethane with triethylphosphite.¹² In the first step the phosphonate ester was prepared. The ester was then converted into the acid by

Table 1. Composition and Color of Cr(II) Organophosphonates

compound	Cr(%)	P(%)	C(%)	H(%)	N(%)	Cl(%)
$\text{Cr}[\text{CH}_3\text{PO}_3]\cdot\text{H}_2\text{O}$ (light-blue)						
found	32.20	17.68	6.15	2.76		
calcd	31.70	18.88	7.32	3.07		
$\text{Cr}[\text{C}_2\text{H}_5\text{PO}_3]\cdot\text{H}_2\text{O}$ (blue)						
found	29.5	16.46	13.83	4.10		
calcd	29.21	17.40	13.49	3.96		
$\text{Cr}_2[(\text{CH}_2)_2(\text{PO}_3)_2]\cdot 3\text{H}_2\text{O}$ (light-blue)						
found	30.40	16.69	7.36	3.12		
calcd	30.23	18.00	6.98	2.93		
$\text{Cr}[\text{NH}_3(\text{CH}_2)_2\text{PO}_3(\text{Cl})]$ (cobalt-blue)						
found	24.65	13.35	11.67	4.19	5.94	15.84
calcd	24.58	14.64	11.36	3.34	6.62	16.76

reacting it with concentrated HCl. Typically, $\text{Br}-(\text{CH}_2)_2-\text{Br}$ (3.76 g, 20 mmol) and $\text{P}(\text{OC}_2\text{H}_5)_3$ (8.31 g, 50 mmol) were refluxed at 150 °C for 6 h under N_2 gas. The solution was then cooled at room temperature, and about 30 mL of concentrated HCl solution (37%) was added. The solution was again heated for 15 h at 100 °C. The solution was cooled at room temperature and 10 mL of water added. The aqueous phase separated and left to evaporate in air at room temperature until a white precipitate is collected (4.0 g, $\approx 90\%$ yield). Satisfactory elemental analyses were obtained. All reactions involving Cr(II) ion were carried out under inert atmosphere by using the usual Schlenck techniques. Water was purged with N_2 gas prior to use. Elemental analyses were performed by Malissa and Reuter Mikroanalytische Laboratorien, Elbach, Germany. Thermogravimetric (TGA) data were collected in flowing dry nitrogen at a rate of 5 °C/min on a Stanton-Redcroft STA-781 thermoanalyzer. X-ray powder diffraction profiles were recorded on a Seifert XRD-3000 diffractometer, with a curved graphite-single-crystal monochromator [$\lambda(\text{Cu K}\alpha) = 1.542 \text{ \AA}$] position-sensitive detector operating in constant scan mode of 0.5 deg/min⁻¹ over the range $3^\circ < 2\theta < 80^\circ$. The sample was mounted on a flat plate under a Mylar sheet, in an N_2 -filled drybox. The diffractometer zero point was determined from an external Si standard. The IR absorption spectra were obtained by using a Perkin-Elmer 621 spectrophotometer by the KBr pellet method. Static magnetic susceptibility measurements were performed by using a Quantum Design MPMS5 SQUID susceptometer in fields up to 5 T. The polycrystalline sample was placed in a Teflon cylinder under nitrogen and sealed and then in a polyethylene straw. All the experimental data were corrected for the core magnetization using Pascal's constants.

Synthesis of Chromium Organophosphonates. $\text{Cr}[\text{RPO}_3]\cdot\text{H}_2\text{O}$, ($\text{R} = \text{CH}_3, \text{C}_2\text{H}_5$). The compounds were prepared by mixing filtered aqueous solutions of alkylphosphonic acid and of CrCl_2 in the presence of urea. The resulting blue solution was kept at 80 °C in an oil bath for a few days. The light-blue microcrystalline precipitate that formed was filtered off under nitrogen, washed several times with degassed water, and then dried under vacuum. The methyl derivative slowly decomposes to the air, while the other one is a very air-sensitive material. The composition of the materials were checked by elemental analyses (see Table 1) and by TGA measurements.

$\text{Cr}_2[\text{O}_3\text{P}-(\text{CH}_2)_2-\text{PO}_3]\cdot 3\text{H}_2\text{O}$. The method of preparation of this compound is similar to that used for the above compounds. Typically, CrCl_2 (3 g, 24.4 mmol) was dissolved in water (15 mL). The solution was filtered and added to a clean water solution containing the ethylenebis(phosphonic acid) (2.26 g, 12.2 mmol) and urea (2.93 g, 49 mmol). The resulting blue solution was heated under nitrogen for a few days at 80 °C. A light-blue powder was separated, washed with water and then with methanol, and dried under vacuum at room temperature. The compound slowly decomposes to the air.

(8) Carling, S. G.; Day, P.; Visser, D.; Kremer, R. K. *J. Solid State Chem.* **1993**, *106*, 111.

(9) (a) Bujoli, B.; Pena, O.; Palvadeau, P.; Le Bideau, J.; Payen, C.; Rouxel, J. *Chem. Mater.* **1993**, *5*, 583. (b) Le Bideau, J.; Payen, C.; Bujoli, B.; Palvadeau, P.; Rouxel, J. *J. Magn. Magn. Mater.* **1995**, *140–144*, 1719.

(10) See for example: Bellitto, C.; Day, P. *J. Mater. Chem.* **1992**, *2*, 265.

(11) Bellitto, C.; Federici, F.; Ibrahim, S. *J. Chem. Soc., Chem. Commun.* **1976**, 759.

(12) Hudson, R. F. *Structure and Mechanism of Organophosphorous Chemistry*; Academic Press: New York, 1965.

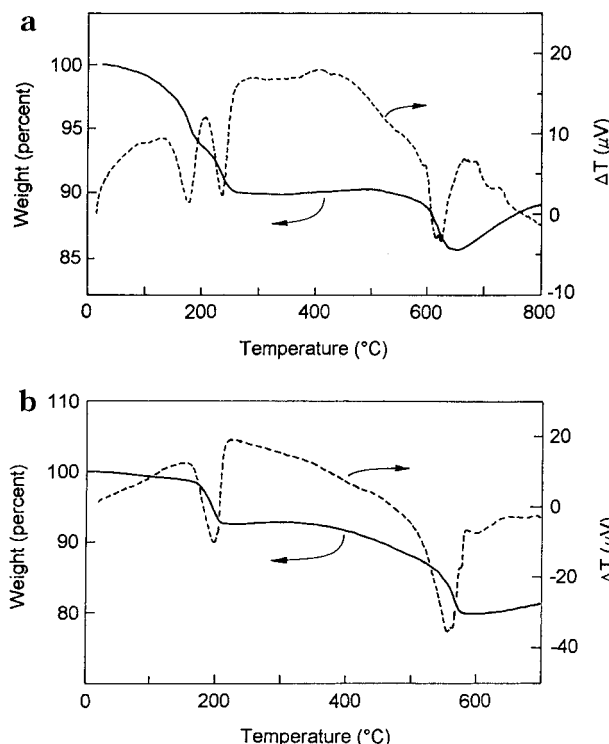


Figure 1. TGA and DSC profiles of (a) $\text{Cr}[\text{CH}_3\text{PO}_3]\cdot\text{H}_2\text{O}$ and of (b) $\text{Cr}[\text{C}_2\text{H}_5\text{PO}_3]\cdot\text{H}_2\text{O}$.

$\text{Cr}[(\text{H}_3\text{N}-(\text{CH}_2)_2-\text{PO}_3)(\text{Cl})]$. CrCl_2 (3.26 g, 26.5 mmol) was dissolved in water (10 mL). The solution was filtered and added to a clean water solution containing the (2-aminoethyl)phosphonic acid (3.31 g, 26.5 mmol) and urea (3.18 g, 53 mmol). The resulting blue solution was heated under nitrogen at 80 °C. After a few days a cobalt-blue microcrystalline powder was separated, which was filtered off, washed with water and methanol, and dried under vacuum at room temperature. The elemental analyses revealed a compound with the unexpected formula of $\text{Cr}[(\text{H}_3\text{N}-(\text{CH}_2)_2-\text{PO}_3)(\text{Cl})]$. The compound decomposes after weeks of exposure to the air.

Results

$\text{Cr}(\text{II})$ organophosphonates have been prepared by the reaction of phosphonic acid and CrCl_2 in water. The preparation was carried out in the presence of urea at a temperature slightly above 80 °C under inert atmosphere. Under these conditions, the urea slowly hydrolyzes with release of ammonia and, therefore, raises the pH of the solution. The color of the compounds varies from light blue to dark blue. The ethyl derivative is very sensitive to the air, while the chromium methylphosphonate and ethylenebis(phosphonate) decompose slowly on exposure to air. Surprisingly, the (2-aminoethyl)phosphonic acid reacts with CrCl_2 to give a compound of formula $\text{Cr}[(\text{H}_3\text{N}-(\text{CH}_2)_2-\text{PO}_3)(\text{Cl})]$. The protonation of the amino group of the phosphonate ligand has been recently observed in $\text{Cu}_{2.5}(\text{H}_3\text{N}-(\text{CH}_2)_2-\text{PO}_3)(\text{OH})_2(\text{SO}_4)$,¹³ and in $\text{Zr}[(\text{H}_3\text{N}-(\text{CH}_2)_2-\text{PO}_3)_2(\text{Cl})_2]$.¹⁴ TGA studies were performed on $\text{Cr}[\text{CH}_3\text{PO}_3]\cdot\text{H}_2\text{O}$, $\text{Cr}[\text{C}_2\text{H}_5\text{PO}_3]\cdot\text{H}_2\text{O}$, $\text{Cr}[(\text{H}_3\text{N}-(\text{CH}_2)_2-\text{PO}_3)(\text{Cl})]$, and $\text{Cr}_2[\text{O}_3\text{P}-(\text{CH}_2)_2-\text{PO}_3]\cdot 3\text{H}_2\text{O}$. The thermogravimetric analysis of $\text{Cr}[\text{CH}_3\text{PO}_3]\cdot\text{H}_2\text{O}$ is reported in Figure 1a

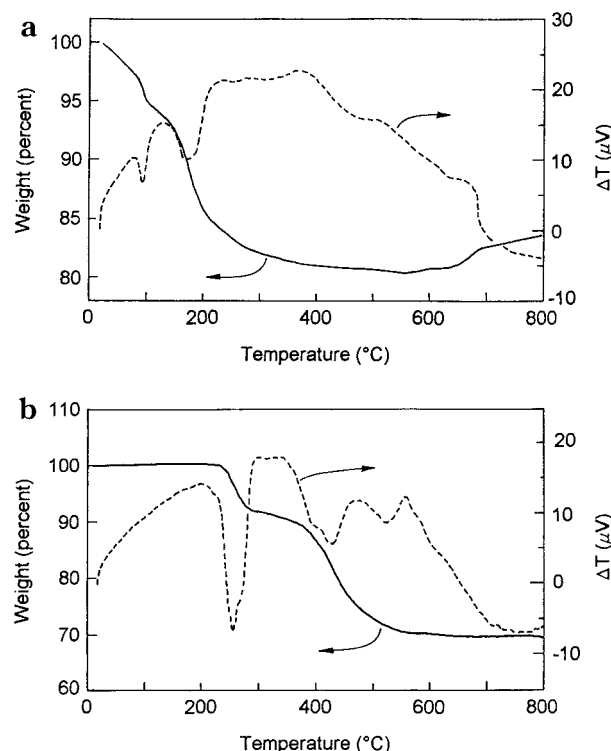


Figure 2. TGA and DSC profiles of (a) $\text{Cr}_2[\text{O}_3\text{P}-(\text{CH}_2)_2-\text{PO}_3]\cdot 3\text{H}_2\text{O}$ and of (b) $\text{Cr}[(\text{H}_3\text{N}-(\text{CH}_2)_2-\text{PO}_3)(\text{Cl})]$.

and it shows three mass losses. The first is at 178 °C (6.16%) and the second one at 238 °C (4.03%). The observed loss of 10.16%, corresponding to this process, is in agreement with the calculated value of 10.97% for the removal of one water molecule per formula unit. The final mass loss is observed between 614 and 622 °C, resulting from the decomposition of the organic ligand, and it is an indication of the high thermal stability of the compound. $\text{Cr}[\text{C}_2\text{H}_5\text{PO}_3]\cdot\text{H}_2\text{O}$ (see Figure 1b) loses water (7.9%) in one stage at 197 °C, and this value is close to the calculated value of 10.1% for the removal of one water molecule. It is instructive to compare the TGA of $\text{Cr}[\text{RPO}_3]\cdot\text{H}_2\text{O}$ to that of $\text{Cu}[\text{CH}_3\text{PO}_3]\cdot\text{H}_2\text{O}$, where the crystal structure has been solved. In the latter, the water molecule is released in one stage at 195 °C and it corresponds to one molecule per formula unit. This is in agreement with the fact that the water molecule is coordinated to copper. The TGA of $\text{Cr}_2[\text{O}_3\text{P}-(\text{CH}_2)_2-\text{PO}_3]\cdot 3\text{H}_2\text{O}$ shows three mass losses (see Figure 2a). The first is between 30 and 60 °C, and it is due to desorption of surface water. The second starts at 90 °C (3.75%), the third starts at 150 °C (10.77%), and the process is complete at 285 °C. The total observed weight loss of 14.52%, in the latter two stages, corresponds to the release of three water molecules per formula unit (calculated value is 15.71%). The first one is due to the removal of one water molecule of crystallization and the latter to the loss of two coordinated water molecules. Above this temperature the compound shows a slight weight loss up to 400 °C and then remains constant up to 600 °C, when the compound starts to decompose. In conclusion, in all these compounds one water molecule is thus coordinated to one chromium ion. $\text{Cr}[(\text{H}_3\text{N}-(\text{CH}_2)_2-\text{PO}_3)(\text{Cl})]$ on the other hand shows no weight loss up to 230 °C, thus suggesting the absence of water molecules in the structure. The

(13) Drumel, S.; Janvier, P.; Bujoli-Doeuff, M.; Bujoli, B. *Inorg. Chem.* **1996**, *35*, 5786.

(14) Rosenthal, G. L.; Caruso, J. *Inorg. Chem.* **1992**, *31*, 3104.

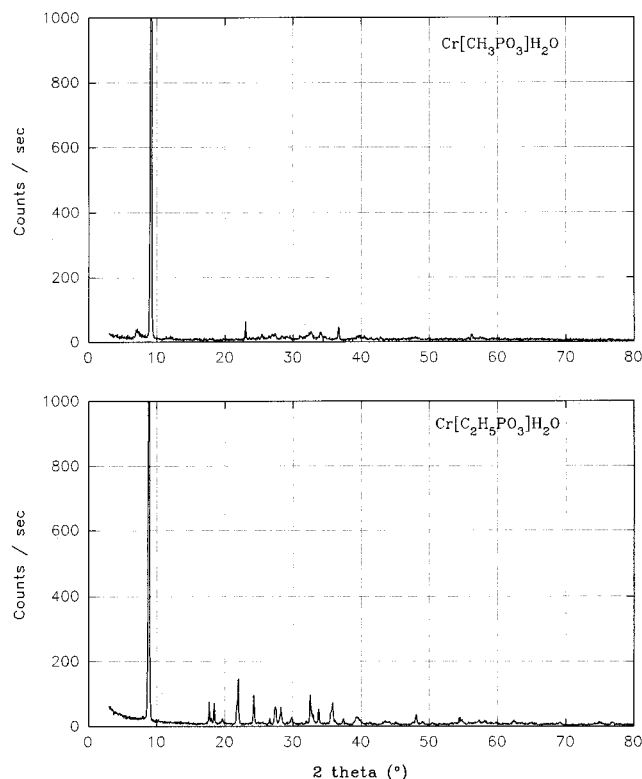


Figure 3. X-ray powder patterns of $\text{Cr}[\text{CH}_3\text{PO}_3]\cdot\text{H}_2\text{O}$ and $\text{Cr}[\text{C}_2\text{H}_5\text{PO}_3]\cdot\text{H}_2\text{O}$.

weight loss of 9.16% starts at about 232 °C, and it continues up to 300 °C. The process continues at much lower rate up to 350 °C, and it stops at 550 °C with a total weight loss of 30% (see Figure 2b).

X-ray Powder Diffraction

$\text{Cr}[\text{CH}_3\text{PO}_3]\cdot\text{H}_2\text{O}$. Figure 3a shows the XRD spectrum of the title compound. Although the spectrum shows well-defined peaks, indicative of an ordered structure, difficulties were found in the indexing, due to being featureless above $2\theta = 40^\circ$. Attempts of fitting were done assuming (1) a rhombohedral space group $R\bar{3}$ of dimensions similar to those observed in a recently reported $\beta\text{-Cu}[\text{CH}_3\text{PO}_3]$ phase^{7a} and (2) an orthorhombic space group found in $\text{Mn}[\text{CH}_3\text{PO}_3]\cdot\text{H}_2\text{O}$.^{4a,8} The results were not distinguishable in accuracy. Attempts to grow a more crystalline sample are in progress.

$\text{Cr}[\text{C}_2\text{H}_5\text{PO}_3]\cdot\text{H}_2\text{O}$. The X-ray powder diffraction pattern is reported in Figure 3b and it was indexed in the monoclinic system with the following unit-cell parameters: $a = 4.86(1) \text{ \AA}$, $b = 10.20(1) \text{ \AA}$, $c = 5.87(1) \text{ \AA}$, and $\beta = 91.0(5)^\circ$. These values are similar to those found for $\text{Mn}[\text{C}_2\text{H}_5\text{PO}_3]\cdot\text{H}_2\text{O}$ ⁸ and $\text{Fe}[\text{C}_2\text{H}_5\text{PO}_3]\cdot\text{H}_2\text{O}$.⁹ The latter crystallize in the monoclinic space group $P1n1$, with unit-cell parameters $a = 4.856(8) \text{ \AA}$, $b = 10.33(1) \text{ \AA}$, $c = 5.744(4) \text{ \AA}$, $\beta = 91.0^\circ$, and $Z = 2$, and it shows a lamellar structure consisting of roughly coplanar layers of iron atoms coordinated octahedrally by five phosphonate oxygen atoms and one water molecule. An attempt to simulate the XRD spectrum by using the same space and the positions of the atoms of $\text{Fe}[\text{C}_2\text{H}_5\text{PO}_3]\cdot\text{H}_2\text{O}$ was done, but the experimental data were only partially reproduced.

$\text{Cr}_2[\text{O}_3\text{P}-(\text{CH}_2)_2-\text{PO}_3]\cdot 3\text{H}_2\text{O}$. The X-ray powder diffraction pattern (see Figure 4) was indexed in the

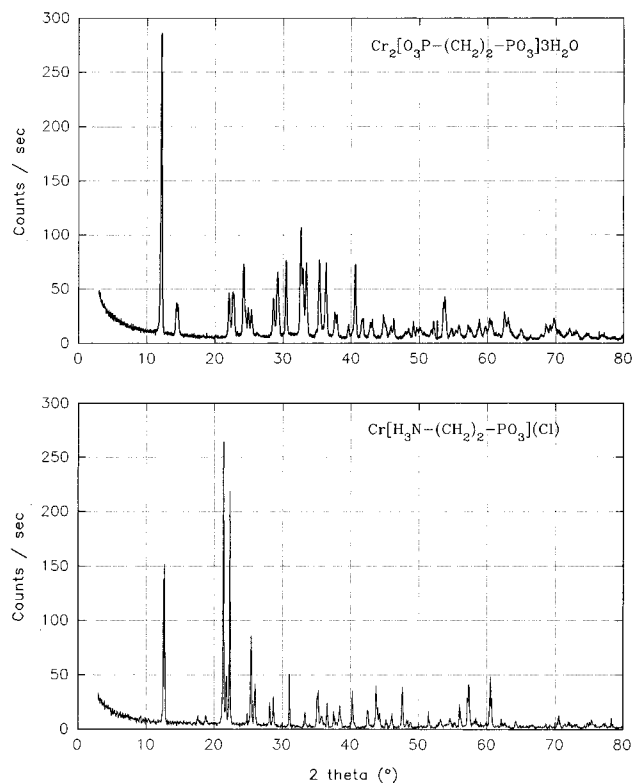


Figure 4. X-ray powder patterns of $\text{Cr}_2[\text{O}_3\text{P}-(\text{CH}_2)_2-\text{PO}_3]\cdot 3\text{H}_2\text{O}$ and $\text{Cr}[\text{H}_3\text{N}-(\text{CH}_2)_2-\text{PO}_3](\text{Cl})$.

monoclinic system with the following unit-cell parameters: $a = 8.08(1) \text{ \AA}$, $b = 7.67(1) \text{ \AA}$, $c = 7.37(1) \text{ \AA}$, and $\beta = 115.0(1)^\circ$. These unit-cell parameters are similar to those reported by Clearfield et al. for $\text{Cu}_2[\text{O}_3\text{P}-(\text{CH}_2)_2-\text{PO}_3(\text{H}_2\text{O})_2]$,¹⁵ the full structure of which has not yet been published. Again, the crystal structure here should be layered, but with adjacent $[\text{Cr}-\text{O}_3\text{P}-\text{C}]$ groups covalently pillared by the $\text{P}-\text{C}-\text{C}-\text{P}$ linkages to create a 3D structure.

$\text{Cr}[(\text{H}_3\text{N}-(\text{CH}_2)_2-\text{PO}_3)(\text{Cl})]$. Figure 4 shows the XRD spectrum of the title compound. An attempt of indexing the X-ray powder diffraction pattern was made by using as starting values the unit-cell parameters found in $\text{Cu}_{2.5}[(\text{H}_3\text{N}-(\text{CH}_2)_2-\text{PO}_3)(\text{OH})_2(\text{SO}_4)]$.¹³ The fitting gave the following unit-cell parameters: $a = 5.43(1) \text{ \AA}$, $b = 20.42(1) \text{ \AA}$, $c = 8.54(1) \text{ \AA}$ and $\beta = 94.0(2)^\circ$. Attempts to grow single crystals for X-ray single-crystal studies are in progress.

Optical Properties

IR Spectra. The IR spectrum of $\text{Cr}[\text{CH}_3\text{PO}_3]\cdot\text{H}_2\text{O}$ is similar to that of $\text{Cu}[\text{CH}_3\text{PO}_3]\cdot\text{H}_2\text{O}$,^{4c} and it is shown in Figure 5a. It features a broad and intense band centered at about 3300 cm^{-1} , assigned as O-H stretch of coordinated water and C-H stretch of the methyl group of the ligand; a band at $1650(\text{m})$ is assigned to H_2O bend, and bands at 1420 and 1314 cm^{-1} are assigned as asymmetric and symmetric C-H deformations, respectively. Four bands due to $[\text{PO}_3]$ group vibrations are observed in the range $1200\text{--}970 \text{ cm}^{-1}$. The infrared spectrum of $\text{Cr}_2[\text{O}_3\text{P}-(\text{CH}_2)_2-\text{PO}_3]\cdot 3\text{H}_2\text{O}$

(15) Poojary, D. M.; Zhang, Y.; Bellingham, P.; Clearfield, A. *Inorg. Chem.* **1996**, *35*, 4942.

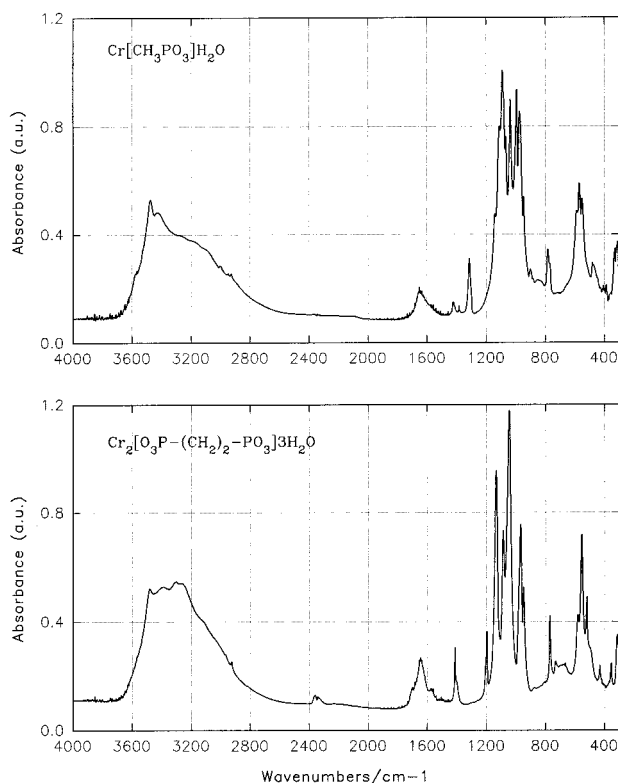


Figure 5. Absorption FTIR spectra of $\text{Cr}[\text{CH}_3\text{PO}_3]\cdot\text{H}_2\text{O}$ and of $\text{Cr}_2[\text{O}_3\text{P}-(\text{CH}_2)_2-\text{PO}_3]\cdot 3\text{H}_2\text{O}$ in the KBr region.

has also been recorded and is reported in Figure 5b. The O–H stretching bands of the water molecules are located between 3250 and 3400 cm^{-1} , while the corresponding deformation is at 1600 cm^{-1} . Bands attributed to the P–O stretching vibrations are in the range 1250 – 970 cm^{-1} by analogy to the assignments previously made for the methyl derivative. The complete conversion of the acid to the salt is demonstrated by the absence of OH stretching of POH group at about 2700 – 2550 and 2350 – 2100 cm^{-1} . Two small overtones at 2903 and 2946 cm^{-1} are the sign of the CH_2 group of the ligand. The IR spectrum of $\text{Cr}[\text{C}_2\text{H}_5\text{PO}_3]\cdot\text{H}_2\text{O}$ is similar to that of the methyl derivative (see Figure 6a). The infrared spectrum of $\text{Cr}[\text{H}_3\text{N}-(\text{CH}_2)_2-\text{PO}_3(\text{Cl})]$ (see Figure 6b) is completely different from those reported above and from that of $\text{Zn}[\text{H}_2\text{N}(\text{CH}_2)_2\text{PO}_3]$.¹⁵ In the former case, the spectrum shows a broad absorption between 2850 and 3300 cm^{-1} which can be assigned to the $-\text{NH}_3^+$ group, indicating that the amine is protonated.¹⁴

UV–Visible Spectra. The diffuse reflectance electronic spectrum of $\text{Cr}[\text{CH}_3\text{PO}_3]\cdot\text{H}_2\text{O}$ has been recorded, and it is reported in Figure 7. It features a very broad band with two maxima at 885 and 643 nm , a shoulder at 338 nm , and an intense peak at 256 nm . This spectrum is compatible with the presence of octahedral $[\text{Cr}^{\text{II}}\text{O}_6]$ chromophore, being similar to the spectrum of the salt $\text{K}_2\text{SO}_4\cdot\text{CrSO}_4\cdot 2\text{H}_2\text{O}$,^{16,17} containing a tetragonally distorted $[\text{Cr}(\text{H}_2\text{O})_6]^{2+}$ ion. Similar spectra have been observed for the other compounds reported in this paper.

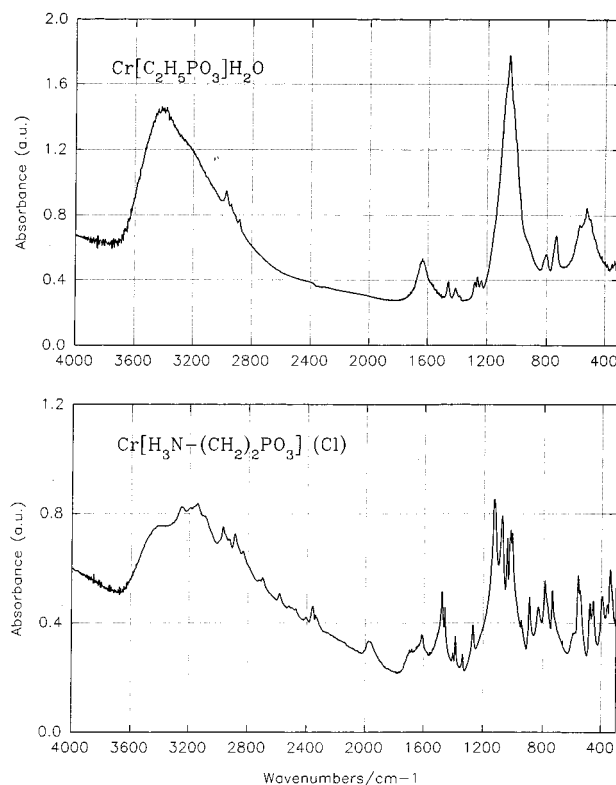


Figure 6. Absorption FTIR spectrum of $\text{Cr}[\text{C}_2\text{H}_5\text{PO}_3]\cdot\text{H}_2\text{O}$ and of $\text{Cr}[\text{H}_3\text{N}-(\text{CH}_2)_2-\text{PO}_3(\text{Cl})]$ in the KBr region.

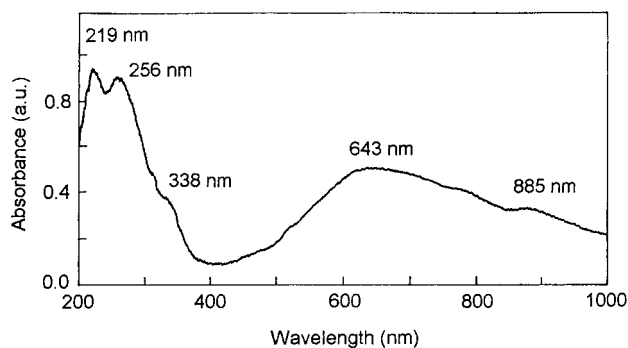


Figure 7. UV–visible reflectance spectra of $\text{Cr}[\text{CH}_3\text{PO}_3]\cdot\text{H}_2\text{O}$.

Magnetic Properties

$\text{Cr}[\text{CH}_3\text{PO}_3]\cdot\text{H}_2\text{O}$. Static magnetic susceptibility measurements were made on samples of different preparations and in fields of 10 and 50 mT from 5 to 300 K . The microcrystalline sample was zero-field cooled to 5 K and the magnetization measured on heating the sample to room temperature. The temperature dependence of the reciprocal of the molar magnetic susceptibility, $1/\chi$, is linear above 100 K , and it follows the Curie–Weiss law (see Figure 8). The Curie constant, C , is $2.92(5)\text{ emu K mol}^{-1}$, as fitted to the high-temperature susceptibility data by using the equation $\chi = N\mu_{\text{eff}}^2/3k_{\text{B}}(T-\theta)$, and this corresponds to an effective magnetic moment of $4.87\text{ }\mu_{\text{B}}$, consistent with the presence of $\text{Cr}(\text{II})$ in a d^4 high-spin configuration. The large negative value of Weiss constant, i.e., $\theta = -230(6)\text{ K}$, indicates strong antiferromagnetic near-neighbor exchange between the adjacent chromium(II) ions. Deviation from Curie–Weiss occurs below 100 K , where the magnetic susceptibility increases until a peak at $T \approx 34\text{ K}$ is observed. This peak can be associated to a

(16) Earnshaw, A.; Larkworthy, L. F.; Patel, K. C.; Beech, G. J. *Chem. Soc. (A)*, **1969**, 1334.

(17) Hand, D. W.; Prout, C. K. *J. Chem. Soc. (A)* **1966**, 168.

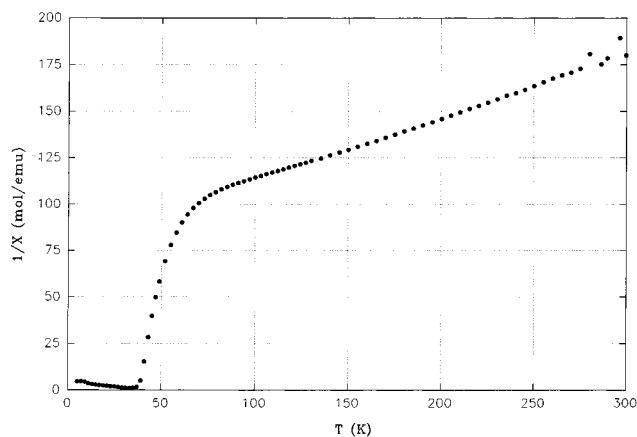


Figure 8. Temperature dependence of the reciprocal of the magnetic susceptibility, $1/\chi$, of polycrystalline $\text{Cr}[\text{CH}_3\text{PO}_3]\cdot\text{H}_2\text{O}$ in the range 5 – 300 K.

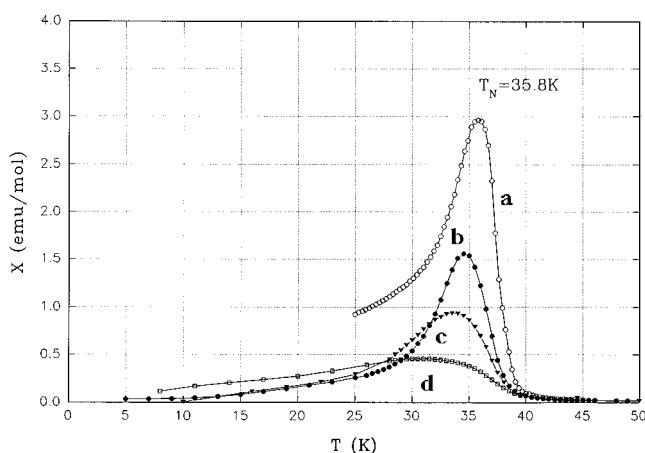


Figure 9. Temperature dependence of magnetic susceptibility, χ , of $\text{Cr}[\text{CH}_3\text{PO}_3]\cdot\text{H}_2\text{O}$ in the temperature range 5 – 60 K at four external applied fields: (a) 100 Oe; (b) 200 Oe; (c) 400 Oe; (d) 1000 Oe.

three-dimensional antiferromagnetic ordering. To obtain a better estimate of the critical temperature, T_N , the experiment was repeated in a lower applied field, and the temperature increased in steps of 0.3 K in the temperature range 25–45 K. The sharpness of the peak increases as well as the susceptibility values ($\chi_{\text{max}} = 2.96$ emu/mol). The value of T_N was found to be 35.8(3) K and the width of the transition of 4 K (see Figure 9). Isothermal magnetization as a function of magnetic field at temperatures below and well above the critical temperature were performed. The magnetic hysteresis loop at $T = 5$ K has also been measured and it is reported in Figure 10. The value of the remnant magnetization, M_r , and coercive field, H_r , are 865 emu G/mol and 2380 Oe, respectively. The isothermal magnetization increases slowly up to a threshold field, H_T , value of 50 mT, where it rises and reaches a maximum value of 1400 emu G/mol at 4 T. This value is 6% of the saturation value expected from an $S = 2$ system, as calculated from the relation

$$M_s = Ngu_B S$$

where N is the Avogadro's number. This corresponds then to the saturation of weak ferromagnetic moments. Hysteresis phenomena disappear at temperatures above

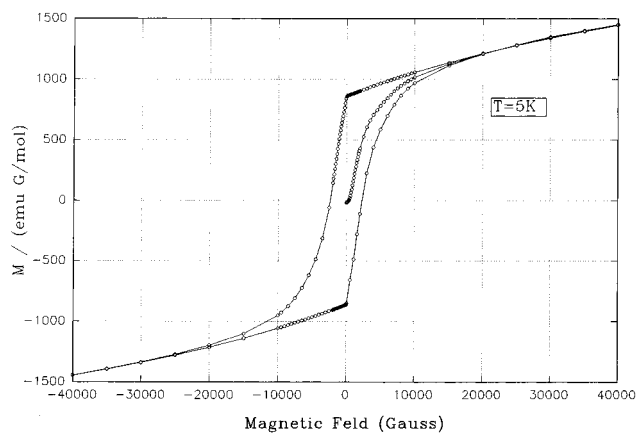


Figure 10. Hysteresis loop for $\text{Cr}[\text{CH}_3\text{PO}_3]\cdot\text{H}_2\text{O}$ at $T = 5$ K.

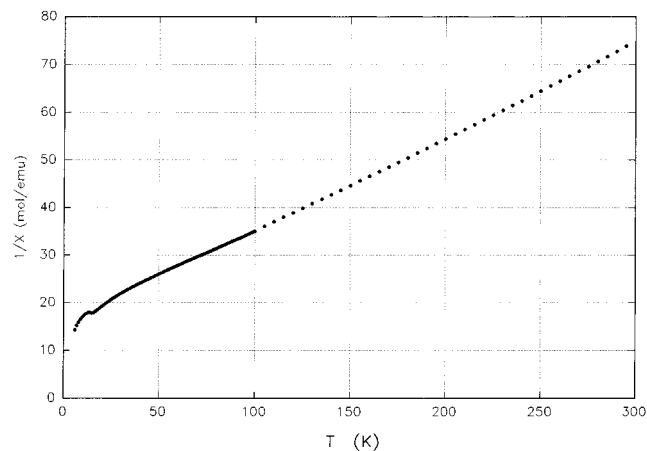


Figure 11. $1/\chi$ vs T plot of polycrystalline $\text{Cr}_2[\text{O}_3\text{P}-(\text{CH}_2)_2-\text{PO}_3]\cdot 3\text{H}_2\text{O}$ in the temperature range 5–300 K.

T_N . At temperatures well above the critical temperature, i.e., at $T = 80$ K, the isothermal magnetization vs field plot is linear, and the C and θ values obtained by the fit were found to be 2.90(5) emu K mol⁻¹ and -230(5) K, thus confirming the high-spin d^4 electronic configuration for the metal ion.

$\text{Cr}_2[\text{O}_3\text{P}-(\text{CH}_2)_2-\text{PO}_3]\cdot 3\text{H}_2\text{O}$. The reciprocal of the molar magnetic susceptibility, $1/\chi$, of the title compound is plotted in Figure 11. At temperatures above 150 K the magnetic data approach the Curie–Weiss behavior, $\chi = C/(T - \theta)$, with the Curie parameter, $C = 5.01(5)$ emu K/mol, corresponding to an effective magnetic moment $\mu_{\text{eff}} = 6.32 \mu_B$ and consistent with the presence of two Cr(II) ions ($S = 2$) per formula unit. The value of the Weiss constant, θ , is large in value and negative, i.e., $\theta = -73$ K, thus indicative of strong antiferromagnetic interactions between the adjacent magnetic ions. Below 100 K, in the χ_m vs T plot, a peak at $T = 15$ K is observed (see Figure 12). $M(H)$ isotherm data up to 4 T were also collected at $T = 6$ K, and the plot was found to be linear.

$\text{Cr}[\text{NH}_3(\text{CH}_2)_2\text{PO}_3(\text{Cl})]$. The molar magnetic susceptibility has been measured in the temperature range 5–70 K. In this range of temperature the magnetic behavior follows the Curie–Weiss law, the Curie constant C being 2.485 emu K mol⁻¹, and the value of the Weiss constant, $\theta = -3$ K as fitted to the high-temperature susceptibility data. This corresponds to an effective magnetic moment of $4.5 \mu_B$, and it is consistent with the presence of Cr(II) ion in a d^4 high-spin

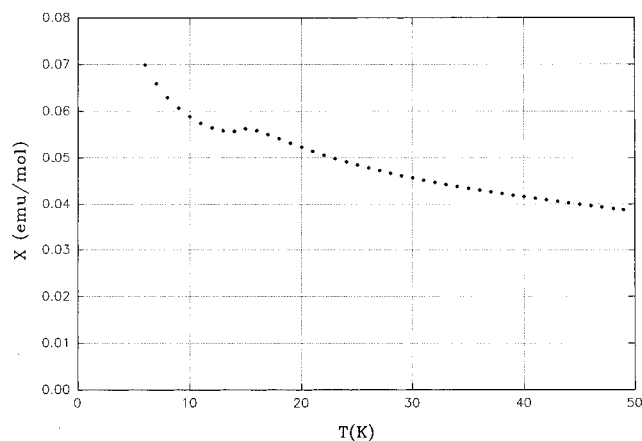


Figure 12. Temperature dependence of magnetic susceptibility, χ , of $\text{Cr}_2[\text{O}_3\text{P}(\text{CH}_2)_2\text{PO}_3]\cdot 3\text{H}_2\text{O}$ in the temperature range 5–50 K.

configuration. An increase of the susceptibility is observed below 6 K.

Discussion

Cr(II) phosphonates have been synthesized and characterized for the first time. The magnetism indicates that the Cr(II) ion is present in the d^4 high-spin configuration. The coordination around the metal ion in $\text{Cr}[\text{CH}_3\text{PO}_3]\cdot\text{H}_2\text{O}$ and in $\text{Cr}_2[\text{O}_3\text{P}-(\text{CH}_2)_2-\text{PO}_3]\cdot 3\text{H}_2\text{O}$ is a distorted octahedron of oxygen atoms. One of the sites is always occupied by the water oxygen, as suggested by the TGA and IR spectra, and five coordinate sites are occupied by the phosphonate oxygen atoms. The scarce crystallinity of the first member of the series and the microcrystallinity of the other derivatives has prevented us, up to now, to know detailed structural information of these solids. Chromium(II) methylphosphonate is an interesting magnetic material. It orders antiferromagnetically at $T_N = 35.8$ K. Although it is difficult to do magneto-structural correlation studies because of the lack of the crystal structure, it is important to point out that the magnetic behavior of this compound is reminiscent of those found in $\text{Mn}[\text{CH}_3\text{PO}_3]\cdot\text{H}_2\text{O}$ ⁸ and in $\text{Fe}[\text{C}_2\text{H}_5\text{PO}_3]\cdot\text{H}_2\text{O}$,⁹ where a lamellar crystal structure is observed. In the latter the iron(II) ions ($S = 2$, $g = 2$) are six-coordinated by five phosphonate oxygen atoms and one water molecule, and they form an irregular two-dimensional inorganic network. This compound orders antiferromagnetically at $T_N = 25$ K, and the antiferromagnetism arises from interactions between nearest neighboring ions that take place via two different 180° Fe–O–Fe superexchange paths. It is likely enough that the chromium salt should have the same layer structure, although it is also difficult to identify in the χ vs T plot any broad maximum above the critical temperature, T_N . Moreover, the calculation of the exchange parameter J/k_B , by using the method of high-temperature series expansion for a 2D system, is prevented by the fact that it is valid only if each magnetic ion is connected to first neighbors, whose couplings are the same both in sign and magnitude. Below T_N , the observed weak ferromagnetism is due to the *spin canting*.²³ In this situation the local spins in the ordered magnetic state are not perfectly parallel, which results in an uncompensated resultant moment in one direction. The canting angle, α , of the Cr^{2+} spins

can be obtained from the relation

$$tg\alpha = \Delta M / Ng\mu_B S$$

where ΔM is the induced magnetization and M_s is the saturation value corresponding to the parallel alignment of all the spins, and here we get $\alpha \approx 3.4^\circ$. The spin canting is indicative of the low symmetry of the ligand field around the open-shell metal ion because only in this situation the so-called antisymmetric exchange²⁴ may occur between neighboring centers and compete with collinear antiferromagnetism. Not many “weak” ferromagnets are reported in the literature,^{8,9,21,22} and they are another category of magnetic solids, having a finite zero-field spontaneous magnetization. The other magnetic salt studied is $\text{Cr}_2[\text{O}_3\text{P}-(\text{CH}_2)_2-\text{PO}_3]\cdot 3\text{H}_2\text{O}$. The compound shows a Curie–Weiss behavior and strong antiferromagnetic interactions between neighboring chromium(II) ions are observed below 100 K. In an attempt to suggest a the structure of this compound several magnetic models have been taken into account and fits of the magnetic susceptibility vs temperature plot were done. A good fit of the plot was obtained, in the range 70–300 K, by assuming the Heiseberg linear-chain model and by using the Smith–Friedberg equation²⁵

$$\chi_{1D} = [Ng^2\mu_B^2 S(S+1)/3k_B T][(1+U)/(1-U)]$$

where $U = \coth K - 1/K$, $K = 2JS(S+1)/k_B T$, and $S = 2$, $g = 2$.

The best value found for J/k_B was -6.7 K. The negative value indicates antiferromagnetic *intrachain* coupling between neighboring Cr(II) ions, and for the fitting that possibly results inside the two-dimensional network, a linear-chain superexchange pathway is preferred. Below 70 K, the susceptibility deviates considerably from the expected behavior for an antiferromagnetic linear chain, and it increases until a maximum at 15 K is reached. The maximum can be interpreted as due to the appearance of *three-dimensional* antiferromagnetic order. Finally, the magnetic behavior of $\text{Cr}[\text{H}_3\text{N}-(\text{CH}_2)_2-\text{PO}_3]$ (Cl) is typical of a paramagnet down to the lowest measured temperature, i.e., 5 K.

Further studies in an attempt to solve the crystal structure of these new solids are in progress.

Acknowledgment. We acknowledge support from Consiglio Nazionale delle Ricerche (Italy) and the Academy of Scientific Research and Technology (Egypt). We would like also to thank Mr. P. Filaci, Mrs. C. Riccucci, and Mr. C. Veroli for technical assistance.

CM970658K

(18) Navarro, R. In *Magnetic Properties of Layered Transition Metal Compounds*; De Jongh, L. J., Ed.; Kluwer Academic Publishers: Dordrecht, Holland, 1990; p 105.

(19) Martinez-Lorente, M. A.; Petrouleas, V.; Savariault, J. M.; Poincot, R.; Drillon, M. *Inorg. Chem.* **1991**, *30*, 3587.

(20) Asaf, U.; Hechel, D.; Felner, I. *Solid State Commun.* **1996**, *98*, 571.

(21) Greedan, J. E.; Reubenbauer, K.; Birchall, T.; Ehlert, M. J. *Solid State Chem.* **1988**, *77*, 376.

(22) Carling, S. G.; Day, P.; Visser, D. *Inorg. Chem.* **1995**, *34*, 3917.

(23) See for example: Carlin, R. L. *Magnetochemistry*; Springer-Verlag: Berlin, 1986; p 149.

(24) Moriya, T. *Phys. Rev.* **1960**, *120*, 91.

(25) Smith, T.; Friedberg, S. A. *Phys. Rev.* **1968**, *176*, 660.